

changes in more general properties, such as firing rates or percentage of complex spikes (fig. S14).

Because early directional firing is stable relative to the environment, it must use environmental cues as well as interoceptive inputs. In addition, directional modulation remains parallel across the whole environment, even during the rat's first-ever exploration of the recording environment (fig. S15A), which indicates that, as in the adult (7), it does not reflect a simple association to a single cue. Furthermore, when tested in two visually different environments, the preferred directions of simultaneously recorded cells rotated together coherently (fig. S15, B and C). These observations suggest the presence of functional sensory input to MEC at P16 and that directional firing could not be produced solely by experience-dependent plasticity driven by movements within the nest before exploration. The timing of development of the different spatial cell types suggests that ontogeny recapitulates phylogeny insofar as the directional signal originates in the brainstem, the place signal originates in archicortex (i.e., hippocampus proper), and the grid cells originate in neo/transcortex.

Stable directional firing, place cell firing, and theta-band temporal organization occur before significant proportions of adultlike grid cells fire. These three factors may combine stable adultlike grid cell firing (15, 16) with further physiological developments [e.g., of MEC stellate cell intrinsic membrane potential oscillations (20)], to create. Once formed, simultaneously recorded grids have similar wavelengths and orientations, as in the adult (6) (fig. S16); these findings are consistent with the presence of coherent ensembles (21). In addition, the appearance of place cell firing with trial-to-trial stability before stable grid cell firing implies that place cell firing can be driven by inputs other than those from grid cells, including environmental inputs, such as boundary vector cells (22–24) or local cues (24), acting together with the (highly stable) directional cells. Our results, together with evidence that place cell firing is not abolished by entorhinal cortex lesions (25), call into question the hypothesis that entorhinal cortex grid cells provide the only spatial input to the place cells. Both place and grid cell firing continues to develop after P20, more rapidly for grid than place cells. Although both systems appear to be interdependent in the adult (26), their differential developmental time courses suggest that interconnectivity develops after pups begin to explore. For example, the presence of theta-modulated firing in both regions at the earliest ages suggests that each area has oscillatory machinery, such as that required for phase precession (16, 27). Controlled rearing studies will be required to further disentangle the dependencies of these different spatial representations on each other and on experiential and innate processes.

Our results put the development of the place and directional systems earlier than previously reported (28) and have general implications for the

interaction of innate and experientially acquired knowledge in spatial cognition. The expression of some types of spatial learning ability continues to improve for a long time after the components of the cognitive map are relatively mature, which suggests that the rate-limiting step may be the use of spatial signals by the rest of the brain. However, some types of spatial behavior in rats, such as spatial orientation based on enclosure geometry (29), are likely directly controlled by head-direction cells, so that our evidence for an early, perhaps preconfigured, directional firing would be consistent with the early appearance of this behavior in humans (30).

References and Notes

1. J. O'Keefe, L. Nadel, *The Hippocampus as a Cognitive Map* (Oxford Univ. Press, Oxford, 1978).
2. F. Schenk, *Behav. Neural Biol.* **43**, 69 (1985).
3. J. W. Rudy, S. Stadler-Morris, P. Albert, *Behav. Neurosci.* **101**, 62 (1987).
4. L. Nadel, L. Wilson, E. M. Kurtz, in *Developmental Time and Timing*, G. Turkewitz and D. A. Devenny, Eds. (Erlbaum, Hillsdale, NJ, 2009), pp. 233–252.
5. J. O'Keefe, J. Dostrovsky, *Brain Res.* **34**, 171 (1971).
6. T. Hafting, M. Fyhn, S. Molden, M. B. Moser, E. I. Moser, *Nature* **436**, 801 (2005).
7. J. S. Taube, R. U. Muller, J. B. Ranck Jr., *J. Neurosci.* **10**, 420 (1990).
8. C. J. Gerrish, J. R. Alberts, *Dev. Psychobiol.* **29**, 483 (1996).
9. Materials and methods are available as supporting material on Science online.
10. W. E. Skaggs, B. L. McNaughton, K. M. Gothard, E. J. Markus, *Adv. Neural Inf. Process. Syst.* **5**, 1030 (1993).
11. C. Barry, R. Hayman, N. Burgess, K. J. Jeffery, *Nat. Neurosci.* **10**, 682 (2007).
12. C. Lever, T. Wills, F. Cacucci, N. Burgess, J. O'Keefe, *Nature* **416**, 90 (2002).
13. J. O'Keefe, M. L. Recce, *Hippocampus* **3**, 317 (1993).
14. T. Hafting, M. Fyhn, T. Bonnevie, M. B. Moser, E. I. Moser, *Nature* **453**, 1248 (2008).
15. N. Burgess, C. Barry, J. O'Keefe, *Hippocampus* **17**, 801 (2007).
16. L. M. Giocomo, E. A. Zilli, E. Fransén, M. E. Hasselmo, *Science* **315**, 1719 (2007).
17. J. Rivas, J. M. Gaztelu, E. García-Austt, *Exp. Brain Res.* **108**, 113 (1996).
18. A. Jeewajee, C. Barry, J. O'Keefe, N. Burgess, *Hippocampus* **18**, 1175 (2008).
19. M. O. Leblanc, B. H. Bland, *Exp. Neurol.* **66**, 220 (1979).
20. B. G. Burton, M. N. Economo, G. J. Lee, J. A. White, *J. Neurophysiol.* **100**, 3144 (2008).
21. B. L. McNaughton, F. P. Battaglia, O. Jensen, E. I. Moser, M. B. Moser, *Nat. Rev. Neurosci.* **7**, 663 (2006).
22. C. Lever, S. Burton, A. Jeewajee, J. O'Keefe, N. Burgess, *J. Neurosci.* **29**, 9771 (2009).
23. T. Solstad, C. N. Boccara, E. Kropff, M. B. Moser, E. I. Moser, *Science* **322**, 1865 (2008).
24. F. Savelli, D. Yoganarasimha, J. J. Knierim, *Hippocampus* **18**, 1270 (2008).
25. T. Van Cauter, B. Poucet, E. Save, *Eur. J. Neurosci.* **27**, 1933 (2008).
26. V. H. Brun et al., *Neuron* **57**, 290 (2008).
27. C. D. Harvey, F. Collman, D. A. Dombeck, D. W. Tank, *Nature* **461**, 941 (2009).
28. P. D. Martin, A. Berthoz, *Hippocampus* **12**, 465 (2002).
29. K. Cheng, *Cognition* **23**, 149 (1986).
30. L. Hermer, E. S. Spelke, *Nature* **370**, 57 (1994).
31. We thank C. Barry for use of adult grid cell data, A. Jeewajee and C. Barry for assistance with data analysis, S. Burton and R. Varriale for technical assistance, and C. Lever and J. Krupic for helpful discussions. This work was supported by the European Union SpaceBrain grant, the Wellcome Trust, the U.K. Medical Research Council, the U.K. Royal Society and a Research Councils U.K. academic fellowship to F.C.

Supporting Online Material

www.sciencemag.org/cgi/content/full/328/5985/1573/DC1
Materials and Methods
SOM Text
Figs. S1 to S16
References

11 February 2010; accepted 22 April 2010
10.1126/science.1188224

Development of the Spatial Representation System in the Rat

Rosamund F. Langston,^{1*†} James A. Ainge,^{1,2*} Jonathan J. Couey,¹ Cathrin B. Canto,¹ Tale L. Bjerknes,¹ Menno P. Witter,¹ Edward I. Moser,^{1‡} May-Britt Moser¹

In the adult brain, space and orientation are represented by an elaborate hippocampal-parahippocampal circuit consisting of head-direction cells, place cells, and grid cells. We report that a rudimentary map of space is already present when 2½-week-old rat pups explore an open environment outside the nest for the first time. Head-direction cells in the pre- and parasubiculum have adultlike properties from the beginning. Place and grid cells are also present but evolve more gradually. Grid cells show the slowest development. The gradual refinement of the spatial representation is accompanied by an increase in network synchrony among entorhinal stellate cells. The presence of adultlike directional signals at the onset of navigation raises the possibility that such signals are instrumental in setting up networks for place and grid representation.

The hippocampus and entorhinal cortex are key components of the brain's network for representing an animal's position in

external space (1, 2). In the hippocampus, place cells fire selectively when the animal visits a specific part of the environment (3). Cortical

inputs to place cells are likely to originate from entorhinal grid cells (4, 5) one or two synapses upstream. These cells have multiple discrete firing locations that, for each cell, define a periodic hexagonal array across the full extent of any space available to the animal (5, 6). Together with head-direction cells and border cells located in the same brain region (7, 8), grid cells are thought to provide the key elements of a path integration-based spatial map in which the animal's position can be updated dynamically in accordance with its own movements (9–11).

The extended ontogenetic development of the hippocampal formation (12) prompted us to ask how space is represented when animals navigate for the first time. Previous work has suggested that, in the juvenile rat, place fields become progressively more adultlike between postnatal days 27 and 50 (P27 to P50) (13), but it has remained unclear whether rat pups form any representation of the local environment at the onset of outbound exploration, between P15 and P20, as would be expected if the spatial representation system is preconfigured (14). We implanted pups with miniature microdrives from the age of P13, generally before the eyelids unsealed (~P14 to P15) (15). The pups were returned to the home cage of their mother after the surgery. Tetrodes were moved toward pre- or parasubiculum, CA1, or medial entorhinal cortex (MEC) over the course of the next 2 to 3 days. Neural activity was then recorded in these regions while the young animals foraged individually in a high-walled square open field (50 cm × 50 cm × 50 cm, or 70 cm × 70 cm × 50 cm). The rat pups covered large segments of the open field from the beginning (fig. S1).

Recordings were first obtained from pre- and parasubiculum, where cells are strongly tuned to head direction in adult rats (16, 17) (Fig. 1A). Directional tuning was quantified by computing, for each recorded cell, the length of the mean vector for the distribution of firing rates across the 360 degrees of possible head directions (15). Cells were classified as direction-modulated if the mean vector length was larger than the 95th percentile of a distribution of mean vector lengths based on shuffled data from the respective brain region and age group. Strong directional tuning was already apparent at P15 and P16 in pups exploring outside the

nest for the first time (26 of 42 cells or 61.9%) (Fig. 1, B to D; fig. S2; and table S1) (12). The fraction of direction-modulated cells at P15 to P16 was substantially larger than expected with random selection from the shuffled distribution [$Z = 16.9$, $P < 0.001$, large-sample binomial test with expected P_0 of 0.05] and not significantly lower than in adult animals (756 out of 1182 pre- and parasubiculum cells, or 64.0%; $Z = 0.916$, $P > 0.15$) (17). The degree of directional tuning was not different from that of head-direction cells in adults [mean vector lengths: 0.679 ± 0.039 and 0.629 ± 0.008 , respectively; $t(777) = 1.10$, $P > 0.25$] (Fig. 1D) (12). The modulation was stable within trials (angular correlation between first and second half: 0.695 ± 0.049) and between trials (0.801 ± 0.087) (12).

We next asked whether hippocampal cells have place fields at the onset of navigational experience. Spatially selective firing was apparent from the outset (Fig. 2; figs. S3 to S5; and

table S2). In the youngest pups (P16 to P18), 24 out of 58 cells (41.4%) satisfied the criteria for place cells (spatial information above the 95th percentile of a distribution for randomly shuffled data from all hippocampal cells in that age group) (Fig. 2C and fig. S6). This is significantly more than expected by random selection from the shuffled distribution ($Z = 25.6$, $P < 0.001$) (Fig. 2D and fig. S6). These early cells were theta-modulated (fig. S7) and showed phase precession (18) and experience-dependent field expansion (19) from the outset (fig. S8). During the 2 weeks after the first exploration session, there was a small and gradual increase in the proportion of place cells (P16 to P24 versus P25 to P35: $Z = 2.80$, $P < 0.005$, binomial test) (Fig. 2, C and D). There was no further increase in information content and coherence in the subpopulation of neurons that passed the criteria for place cells ($r < 0.14$, $P < 0.05$) (Fig. 2E), but firing fields generally became more stable, both within and between trials

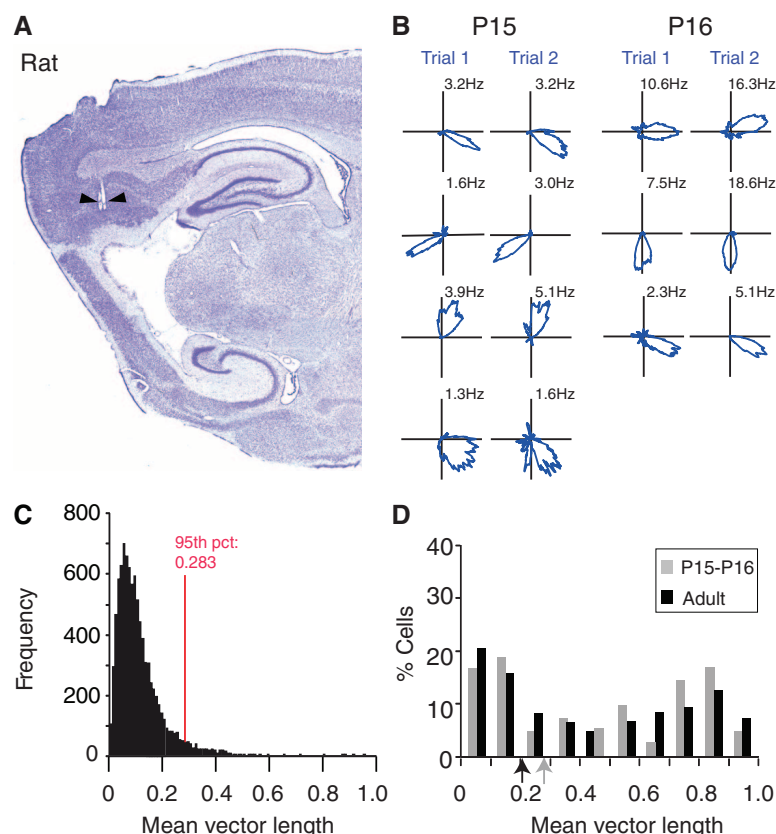


Fig. 1. Head-direction cells during first-time navigation. (A) Nissl-stained sagittal brain section showing representative recording location (arrowhead) in dorsal presubiculum. (B) Strong directional tuning of presubiculum cells on postnatal days P15 and P16. Traces show firing rate as a function of head direction on two trials. Postnatal day and peak firing rate are indicated. (C) Distribution of mean vector lengths (directional tuning) across 16,800 sets of randomly shuffled data from all P15 to P16 cells. Red line indicates 95th percentile (chance level). (D) Frequency distribution showing mean vector lengths in observations from pre- and parasubiculum cells at P15 to P16 (gray) and adult age (black). Arrows indicate chance levels [determined as in (C)].

¹Kavli Institute for Systems Neuroscience and Centre for the Biology of Memory, Medical Technical Research Center, Norwegian University of Science and Technology, Olav Kyrres gate 9, 7489 Trondheim, Norway. ²School of Psychology, University of St. Andrews, St. Mary's Quad, South Street, St. Andrews, Fife KY16 9JP, Scotland.

*These authors contributed equally to this work.

†Present address: Centre for Neuroscience, Division of Medical Sciences, Ninewells Hospital and Medical School, Dundee DD1 9SY, Scotland, UK.

‡To whom correspondence should be addressed. E-mail: edvard.moser@ntnu.no

[spatial correlation versus age: $r(159) = 0.272$, $P < 0.001$ and $r(137) = 0.356$, $P < 0.001$, respectively] (Fig. 2F). The changes could not be attributed merely to differences in behavior (fig. S1) and appeared to be more related to age than to the number of training trials (12). There was no difference between any of the spatial firing measures in the oldest group of juveniles (P31 to P35) and those of the adult group ($P > 0.05$).

The presence of spatially selective firing in CA1 of rat pups was mirrored in recordings from superficial layers of MEC, at positions known to contain large numbers of grid cells in adult rats (4–7) (Fig. 3; figs. S4, S9, and S10; and table S3). Cells with multi-peaked firing fields were observed from the onset of exploration at P16 to P18, but these fields often lacked the strict periodicity of adult grid cells (Fig. 3B and fig. S9). Eleven out of 86 cells recorded in MEC at P16 to P18 (12.8%) passed the criterion for grid cells (rotational-symmetry scores exceeding the 95th percentile of a distribution of grid scores for shuffled data from all MEC cells of the respective age group; Fig. 3, C and D; and figs. S11 and S12). This is significantly more than expected by random selection from the shuffled distribution ($Z = 3.31$, $P < 0.001$) (Fig. 3D, figs. S12 and S13) (12). The fraction of cells that satisfied the grid-score criterion showed no significant change between the first and second block of 10 days (P16 to P25 versus P26 to P34: $Z = 1.03$, $P > 0.15$, Fig. 3, C and D) but increased between the young groups (P16 to P34) and the adults ($Z = 2.50$, $P < 0.01$). The periodic properties of the early gridlike cells evolved noticeably during the first 2 weeks of outbound exploration (Fig. 3, B and E). In the juvenile groups (P16 to P34), there was a significant age-related increase in grid scores within the population of cells that passed the criterion [$r(46) = 0.358$, $P = 0.01$] (figs. S9 and S12). There was no further increase in the grid scores of the grid cells after 4 weeks of age [P28 to P34 versus adults: $t(25) = 0.80$, $P > 0.40$]. The enhancement of spatial periodicity was accompanied by a growing number of theta-modulated neurons (fig. S7), as well as improved spatial stability of entorhinal firing fields [within trials: $r(319) = 0.236$, $P < 0.001$; between trials: $r(226) = 0.374$, $P < 0.001$] (Fig. 3F).

We asked if the entorhinal representation of young animals is directionally modulated, considering that most cells in layer III of the adult MEC have directional preferences (7). Twenty of the 86 entorhinal cells in the P16 to P18 group (23.3%) passed the criterion for direction-modulated cells (Fig. 3H and fig. S14). This is significantly more than expected by random selection from the shuffled distribution ($Z = 7.77$, $P < 0.001$, large-sample binomial test with expected P_0 of 0.05) (Fig. 3G and figs. S12 and S15). There was no further

change in the proportion of direction-modulated neurons across age groups (P16 to P24 versus P25 to P34: $Z = 1.92$, $P > 0.05$) (Fig. 3H) but the tuning of those cells that satisfied the criterion became stronger [age versus mean vector length: $r(104) = 0.344$, $P < 0.001$; age versus directional information: $r(104) = 0.387$, $P < 0.001$] (Fig. 3I), and there was a significant increase in angular correlation within and between trials [$r(320) = 0.184$, $P = 0.001$ and $r(226) = 0.374$, $P < 0.001$, respectively, all MEC cells] (12) (Fig. 3J).

The gradual fine-tuning of the spatial and directional representation in MEC suggests that this network is still developing when rats explore the external world for the first time. To

probe the maturity of the spatial representation circuit more directly, we made simultaneous whole-cell recordings from groups of three or four unconnected medial entorhinal stellate cells in horizontal brain slices from pups of the same litters as used for the in vivo study (Fig. 4A). Spontaneous subthreshold changes in membrane potential were then correlated across cell pairs (Fig. 4, B and C). At P16 to P21, significant correlations in membrane potential were observed during ~10% of the total time sampled. This percentage increased to 29% at P22 to P24 and remained at 30 to 40% at P25 to P29 [$F(4,101) = 20.2$, $P < 0.001$] (12). In contrast to the intrinsic MEC connections, the strong external inputs to layer II/III cells

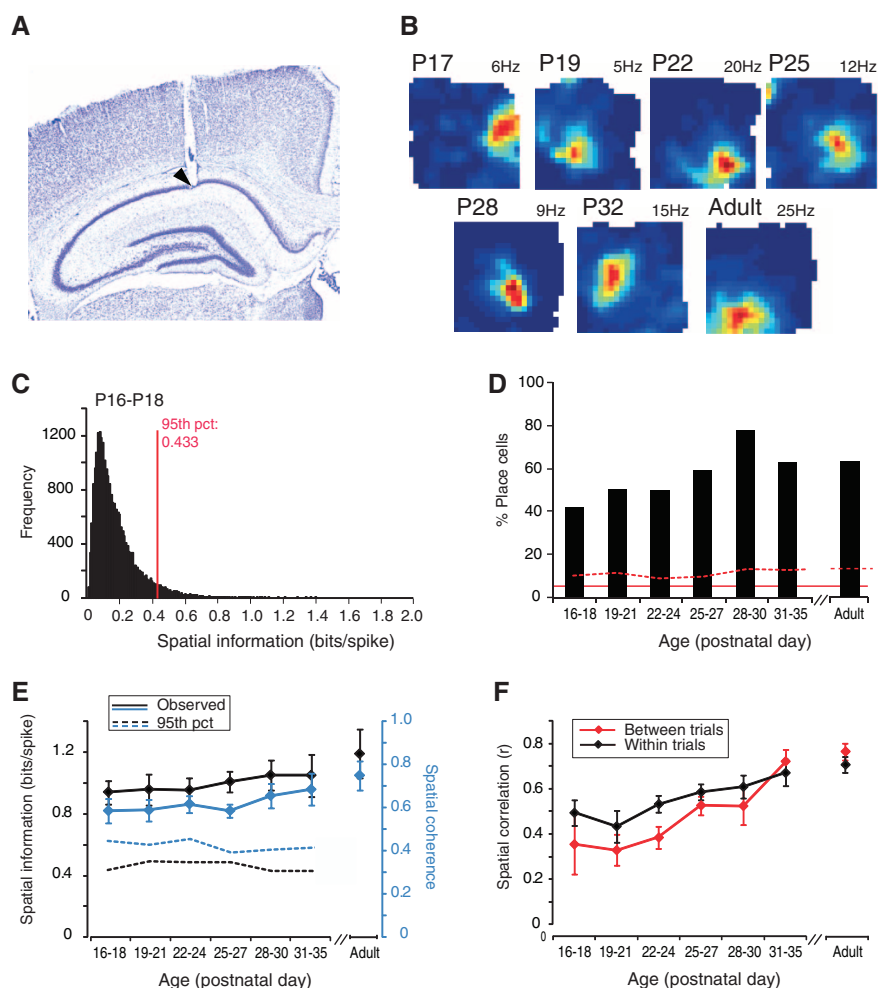


Fig. 2. Development of place cells. (A) Nissl-stained coronal brain section showing representative tetrode location in CA1. (B) Firing fields of CA1 place cells between P17 and P35. Rate maps are color-coded from blue to red; maximal rate is indicated. (C) Distribution of spatial information scores across 23,200 sets of randomly shuffled data from P16 to P18. Red line indicates 95th percentile. (D) Percentage of hippocampal cells passing the 95th percentile criterion for place cells in each age block. Red solid line indicates the proportion of cells, P_0 , expected to pass the criterion in (C) by chance (5%). Red stippled line indicates upper limit of 95% confidence interval for P_0 . (E) Spatial information (black) and spatial coherence (blue) as a function of age (means \pm SEM; all hippocampal place cells). (F) Spatial correlation between rate maps on first and second half of each trial and between consecutive trials (all active CA1 cells).

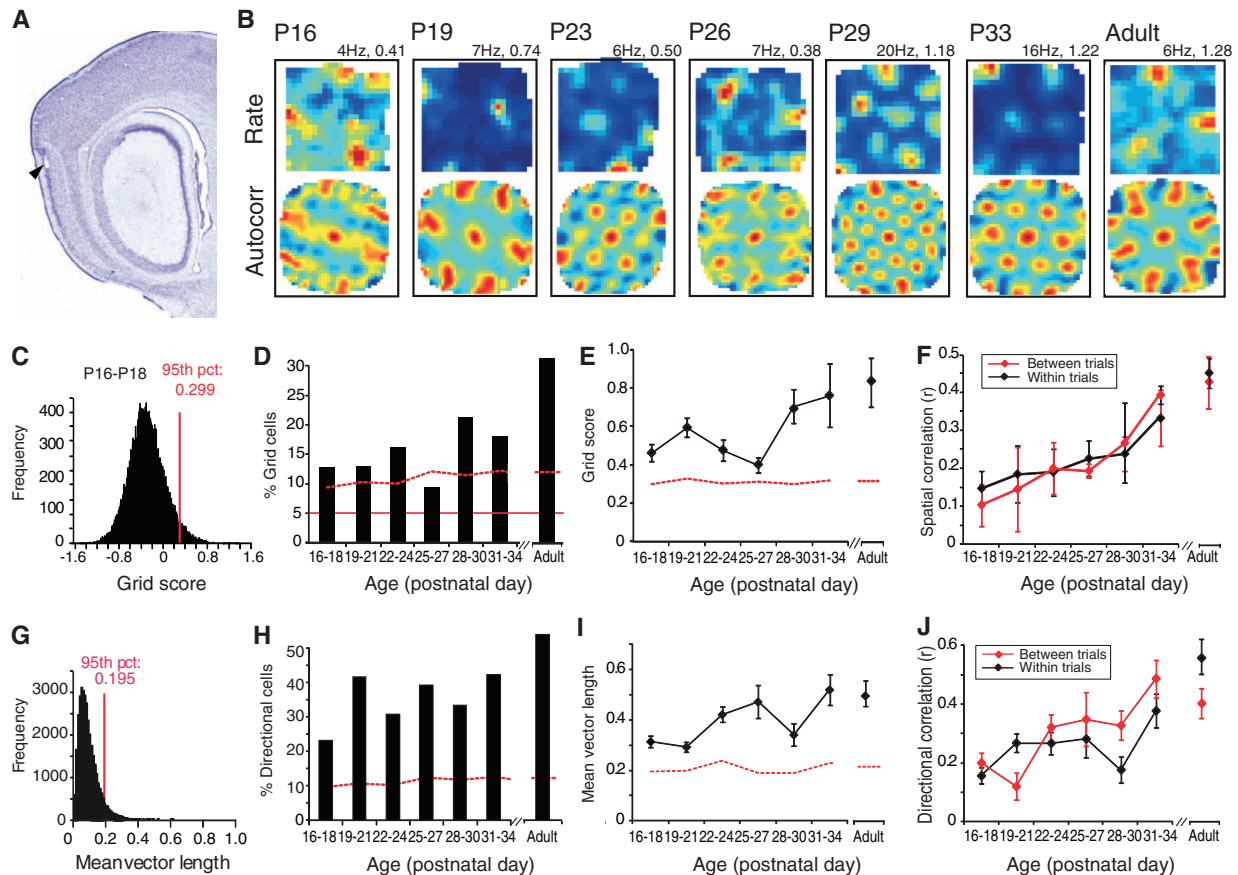
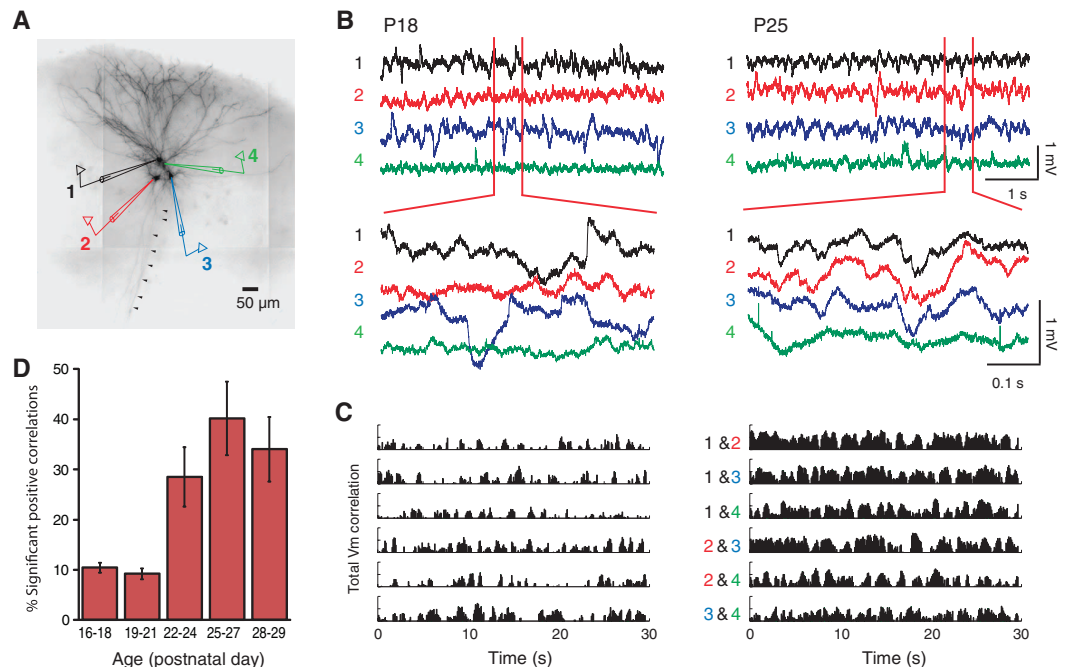


Fig. 3. Development of grid cells. (A) Nissl-stained sagittal brain section showing representative recording position in layer II of MEC. (B) Firing fields of entorhinal grid cells from P16 to P34: (top) rate maps, as in Fig. 2B; (bottom) spatial autocorrelations, color scale from blue ($r = -1$) to red ($r = +1$), grid scores are indicated. (C) Distribution of grid scores across 32,400 sets of shuffled data from P16 to P18. Red line indicates 95th percentile. (D) Percentage of cells that passed the 95th percentile criterion in (C). Solid and stippled lines as in Fig. 2D. (E) Grid

scores as a function of age (grid cells only; means \pm SEM). (F) Spatial correlation between rate maps (means \pm SEM; all entorhinal cells, as in Fig. 2F). (G) Distribution of mean vector lengths across 34,400 sets of randomly shuffled data from all MEC cells. (H) Percentage of MEC cells with mean vector lengths above the chance level. (I) Mean vector length as a function of age (direction-modulated cells only; means \pm SEM). (J) Stability of directional tuning as a function of age (angular correlations, all entorhinal cells; means \pm SEM).

Fig. 4. Age-dependent synchrony in subthreshold membrane potential between layer II stellate cells. (A) Representative experimental setup. Four layer II stellate cells were filled with biocytin on P18; cell number is indicated by color; colors correspond to traces in (B and C). Arrowheads indicate descending axons. (B) Resting-membrane potential traces in four simultaneously recorded stellate cells from P18 and P25. Traces are shown at two time scales (upper versus lower). (C) Membrane voltage (V_m) correlation between sets of four cells at P18 and P25 measured over 30 s. Each row shows the correlation across time between the membrane voltage of one pair of cells (identities indicated with numbers and color in the center). Correlation values were calculated using a 250-ms sliding window moved in 50-ms increments. Only positive correlations are shown. (D) Percentage of significant positive correlations ($P < 0.001$) per age group (mean \pm SEM).



from the presubiculum and parasubiculum (20) already had adultlike properties at 2 weeks of age (fig. S16). The stabilization of entorhinal and hippocampal spatial representations at about 3½ to 4 weeks of age largely coincides with the emergence of adultlike connectivity within the entorhinal microcircuit, which suggested that local network synchrony is instrumental in forming an accurate and precisely updated metric representation of self-position (9, 10).

Our study has two main findings. First, head-direction cells, place cells, and grid cells were detected when rat pups navigated spaces outside the nest for the first times in their lives. The three cell types may interact from the outset, with rudimentary grid cells providing sufficiently patterned input to the hippocampus to generate place-specific firing in this region (9, 10, 21, 22). Second, directional and positional components of the representation were found to mature at different rates. Head-direction cells in pre- and parasubiculum showed adultlike properties when the pups left the nest for the first time, often only hours after the eyelids had unsealed, whereas grid and place cells continued to evolve, with many grid cells not reaching adultlike levels of spatial periodicity until about 4 weeks of age. Because connections from pre- and parasubiculum to MEC were already functional at P16, the early representation of direction in pre- and parasubiculum may be instrumental in the subsequent development

of adultlike grid and place maps in entorhinal cortex and hippocampus. The evolution of functional intrinsic connections in MEC during the fourth week may be essential not only for grid formation but also for reliable translation of the representation across the network in response to ongoing changes in the animal's speed and direction (9, 10). Whether the formation of prototypical representations in the parahippocampal and hippocampal cortices requires translational or vestibular experience at younger ages, in the nest, remains to be determined.

References and Notes

1. J. O'Keefe, L. Nadel, *The Hippocampus as a Cognitive Map* (Clarendon Press, Oxford, 1978).
2. E. I. Moser, E. Kropff, M.-B. Moser, *Annu. Rev. Neurosci.* **31**, 69 (2008).
3. J. O'Keefe, J. Dostrovsky, *Brain Res.* **34**, 171 (1971).
4. M. Fyhn, S. Molden, M. P. Witter, E. I. Moser, M.-B. Moser, *Science* **305**, 1258 (2004).
5. T. Hafting, M. Fyhn, S. Molden, M.-B. Moser, E. I. Moser, *Nature* **436**, 801 (2005).
6. M. Fyhn, T. Hafting, A. Treves, M.-B. Moser, E. I. Moser, *Nature* **446**, 190 (2007).
7. F. Sargolini *et al.*, *Science* **312**, 758 (2006).
8. T. Solstad, C. N. Boccara, E. Kropff, M.-B. Moser, E. I. Moser, *Science* **322**, 1865 (2008).
9. M. C. Fuhs, D. S. Touretzky, *J. Neurosci.* **26**, 4266 (2006).
10. B. L. McNaughton, F. P. Battaglia, O. Jensen, E. I. Moser, M.-B. Moser, *Nat. Rev. Neurosci.* **7**, 663 (2006).
11. N. Burgess, C. Barry, J. O'Keefe, *Hippocampus* **17**, 801 (2007).
12. Supporting text and figures are available as supporting material on Science Online.
13. P. D. Martin, A. Berthoz, *Hippocampus* **12**, 465 (2002).
14. I. Kant, *Kritik der reinen Vernunft* (J. F. Hartknoch, Riga, Latvia, 1781).
15. Materials and methods are available as supporting material on Science Online.
16. J. S. Taube, R. U. Muller, J. B. Ranck Jr., *J. Neurosci.* **10**, 420 (1990).
17. C. N. Boccara *et al.*, *Soc. Neurosci. Abstr.* **34**, 94.9 (2008), presented 15 November 2008.
18. J. O'Keefe, M. L. Recce, *Hippocampus* **3**, 317 (1993).
19. M. R. Mehta, C. A. Barnes, B. L. McNaughton, *Proc. Natl. Acad. Sci. U.S.A.* **94**, 8918 (1997).
20. M. Caballero-Bleda, M. P. Witter, *Exp. Brain Res.* **101**, 93 (1994).
21. T. Solstad, E. I. Moser, G. T. Einevoll, *Hippocampus* **16**, 1026 (2006).
22. E. T. Rolls, S. M. Stringer, T. Elliot, *Network* **17**, 447 (2006).
23. We thank R. Skjerpeng for programming; C. N. Boccara for sharing adult pre- and parasubiculum data; and A. M. Amundsgård, K. Haugen, K. Jenssen, H. Waade, and T. Åsmul for technical assistance. Supported by Fondation Bettencourt-Schueller, Seventh Framework Programme of the European Commission (SPACEBRAIN), Kavli Foundation, and a Centre of Excellence grant from the Research Council of Norway.

Supporting Online Material

www.sciencemag.org/cgi/content/full/328/5985/1576/DC1
Materials and Methods
SOM Text
Figs. S1 to S16
Tables S1 to S3
References

10 February 2010; accepted 22 April 2010
10.1126/science.1188210